

**HYPERANALYTIC DUAL TREE COMPLEX WAVELET
TRANSFORM BASED IMAGE DENOISING USING BI-
VARIATE SHRINKAGE FILTER**

S. Swarnalatha^{*}

Dr. P. Satyanarayana^{**}

B. Shoban Babu^{***}

ABSTRACT:

This paper emphasizes the improvement in the denoising capability of the new proposed technique 'Hyperanalytic Dual Tree Complex Wavelet Transform (HDTTCWT)'. This technique combines the merits of both Hyperanalytic Wavelet Transform (HWT) and Dual Tree Complex Wavelet Transform (DTCWT). Bi-variate shrinkage Filtering excels in estimating the signal from the noisy signals. The proposed wavelet transform performs better than the HWT and DTCWT based image denoising techniques.

Keywords: Discrete Wavelet Transform (DWT), Dual Tree Complex Wavelet Transform (DTCWT), Hyperanalytic Wavelet Transform (HWT), Hyperanalytic Dual Tree Complex Wavelet Transform (HDTTCWT), Bi-variate shrinkage filter.

^{*} Associate Professor, Dept. of E.C.E., S.V.U.C.E., Tirupati. A.P, India.

^{**} Professor, Dept. of E.C.E., A.I.T.S, Tirupati, A.P, India.

^{***} Associate Professor, Dept. of E.C.E., S.V.C.E.T., Chittoor, A.P, India.

I. Introduction

The wavelet transform is a simple and elegant tool that can be used for many digital signal and image processing applications. It overcomes some of the limitations of the Fourier transform with its ability to represent a function simultaneously in the frequency and time domains using a single prototype function (or wavelet) and its scales and shifts. The wavelet transform comes in several forms. The critically-sampled form of the Discrete Wavelet Transform (DWT) provides the most compact representation; however, it has several limitations. For example, it lacks the shift-invariance property, and in multiple dimensions it does a poor job of distinguishing orientations, which is important in image processing. For these reasons, it turns out that for some applications, improvements can be obtained by using an expansive wavelet transform in place of a critically-sampled one. An expansive transform is one that converts an N -point signal into M coefficients with $M > N$. The dual-tree complex wavelet transform overcomes these limitations, it is nearly shift-invariant and is oriented in 2-D. The 2-D Dual Tree Complex Wavelet Transform (DTCWT) reduces six sub-bands at each scale, each of which is strongly oriented at distinct.

Analytic Discrete Wavelet Transform (ADWT) is also a complex wavelet transform which is free from the poor shift sensitivity and poor directionality. ADWT is realized by converting the signal to a complex signal through Hilbert Transform and computing real DWT for the complex signal. Two dimensional ADWT is named as Hyperanalytic Wavelet Transform (HWT). Like DTCWT, HWT also produces six distinct sub-bands at each scale. Analytic Dual Tree Complex Wavelet Transform (ADTCWT) is an extension of the ADWT, and it obtained by mixing the features of the ADWT and DTCWT. Hyperanalytic Dual Tree Complex Wavelet Transform (HDTCWT) is the 2D version of the ADTCWT.

II. Different Wavelet Transforms

II (a).Discrete wavelet transform (DWT)

Mathematically the Discrete wavelet transform pair for one dimensional can be defined as

$$W_{\phi}(j_0, k) = \frac{1}{\sqrt{M}} \sum_{x=0}^{M-1} f(x) \tilde{\phi}_{j_0, k}(x) \dots \dots \dots (1)$$

$$W_{\psi}(j_0, k) = \frac{1}{\sqrt{M}} \sum_{x=0}^{M-1} f(x) \tilde{\psi}_{j_0, k}(x) \dots \dots \dots (2)$$

for $j \geq j_0$ and

$$f(x) = \frac{1}{\sqrt{M}} \sum_k W_{\phi}(j_0, k) \phi_{j_0, k}(x) + \frac{1}{\sqrt{M}} \sum_{j=j_0}^{\infty} \sum_k W_{\psi}(j, k) \psi_{j, k}(x) \dots \dots \dots (3)$$

Where $f(x), \phi_{j_0, k}(x), \psi_{j, k}(x)$ are future function of discrete variable $x=0,1,2,3, \dots$

In two dimensions, a two-dimensional scaling function, $\phi(x, y)$, and three two-dimensional wavelet $\psi^H(x, y), \psi^V(x, y)$ and $\psi^D(x, y)$ are required.

Each is the product of a one-dimensional scaling function ϕ and corresponding wavelet ψ .

$$\phi(x, y) = \phi(x)\phi(y) \dots \dots \dots (4)$$

$$\psi^H(x, y) = \psi(x)\phi(y) \dots \dots \dots (5)$$

$$\psi^V(x, y) = \phi(x)\psi(y) \dots \dots \dots (6)$$

$$\psi^D(x, y) = \psi(x)\psi(y) \dots \dots \dots (7)$$

where ψ^H measures variations along columns (like horizontal edges), ψ^V responds to variations along rows (like vertical edges), and ψ^D corresponds to variations along diagonals.

1-D Filter Bank: The 1-D filter bank is constructed with analysis and synthesis filter bank. The analysis filter bank decomposes the input signal $x(n)$ into two sub band signals, $c(n)$ and $d(n)$. The signal $c(n)$ represents the low frequency part of $x(n)$, while the signal $d(n)$ represents the high frequency part of $x(n)$.

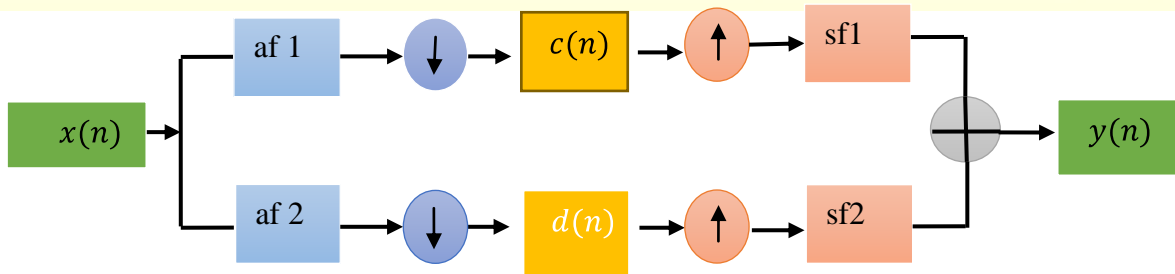


Fig. 1. The Analysis filter bank Fig. 2. The Synthesis filter bank

We have denoted the low pass filter by af1 (analysis filter 1) and the high pass filter by af2 (analysis filter 2). As shown in the Fig. 1, the output of each filter is then down sampled by 2 to obtain the two sub band signals $c(n)$ and $d(n)$ [1] [2-4]. The Synthesis filter bank combines the two sub band signals $c(n)$ and $d(n)$ to obtain a single signal $y(n)$. The synthesis filters bank up-samples each of the two sub band signals. The signals are then filtered using a low pass and a high pass filter. We have denoted the low pass filter by sf1 (synthesis filter1) and the high pass filter by sf2 (synthesis filter 2) as shown in the Fig. 2. The signals are then added together to obtain the signal $y(n)$. If the four filters are designed so as to guarantee that the output signal $y(n)$ equals the input signal $x(n)$, then the filters are said to satisfy the perfect reconstruction condition [1][2-4].

2-D Filter Banks: To use the wavelet transform for image processing we must implement a 2-D version of the analysis and synthesis filter banks. In the 2-D case, the 1-D analysis filter bank is first applied to the columns of the image and then applied to the rows. If the image has N_1 rows and N_2 columns, then after applying the 1-D analysis filter bank to each column we have two sub-band images, each having $N_1/2$ rows and N_2 columns; after applying the 1-D analysis filter bank to each row of both of the two sub-band images, we have four sub-band images, each having $N_1/2$ rows and $N_2/2$ columns. This is illustrated in figure 3. The 2-D synthesis filter bank combines the four sub-band images to obtain the original image [1] [2-4].

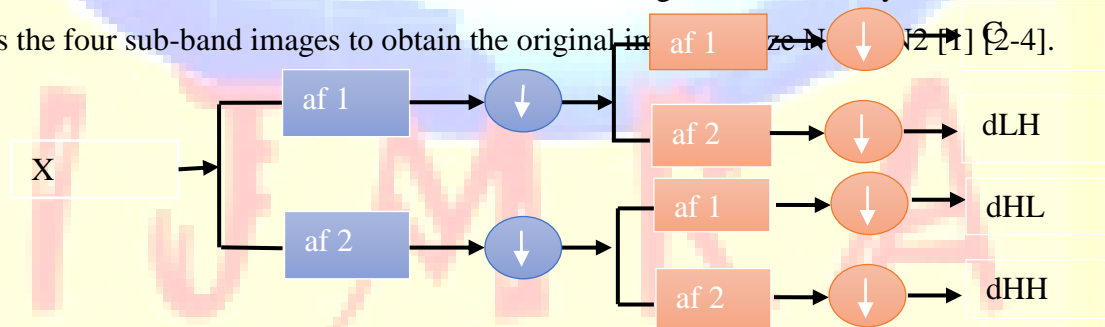


Fig. 3. One stage in multi-resolution wavelet decomposition of an image

The two-dimensional DWT can be implemented using digital filters and downsamplers and it is shown in the Figs. 4 & 5 respectively

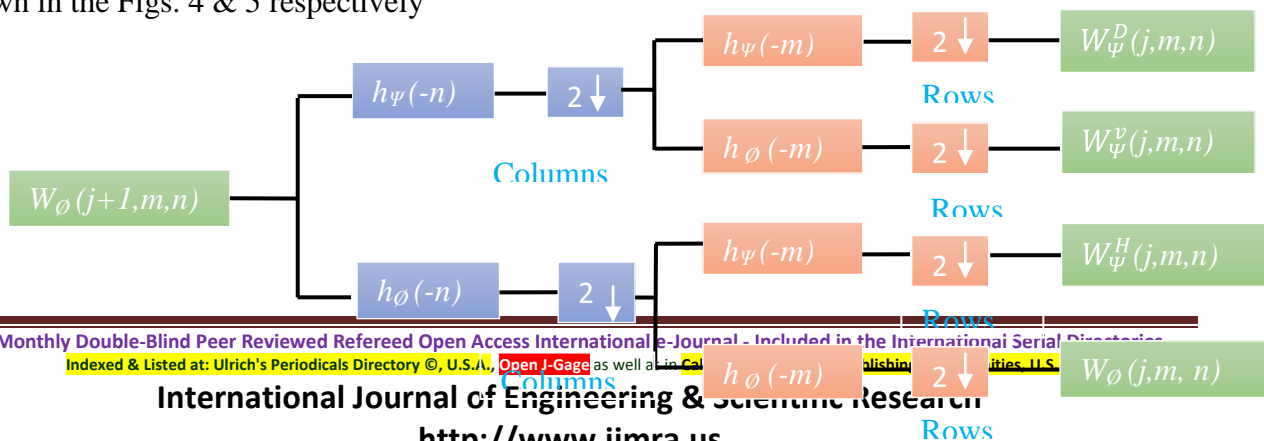


Fig. 4. The two-dimensional DWT the analysis filter

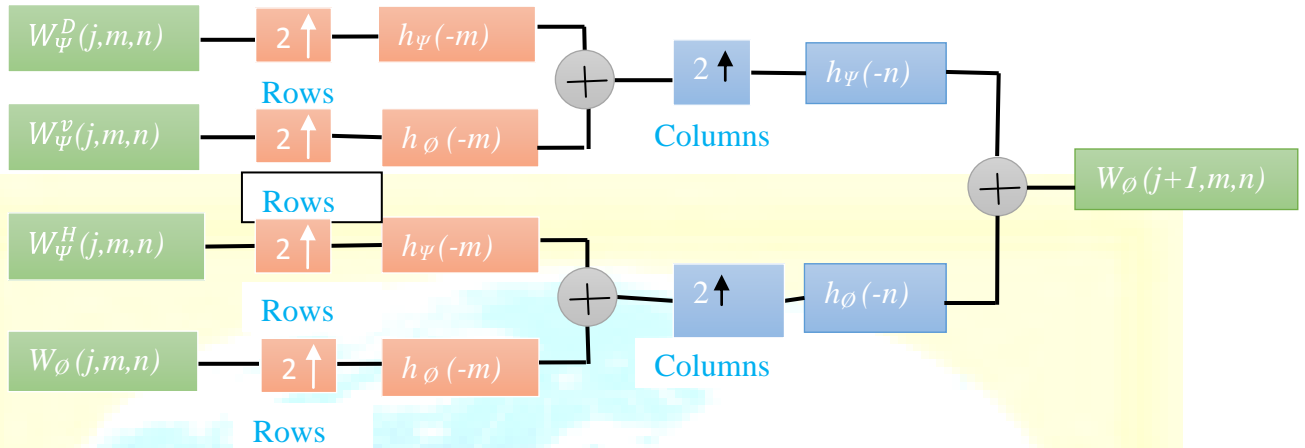


Fig. 5. The two-dimensional DWT the synthesis filter

Limitations of DWT

Although the standard DWT is a powerful tool, it has three major disadvantages that undermine its application for certain signal and image processing tasks [5]. These disadvantages [6] [7] are

1. Shift Sensitivity

A transform is shift sensitive, if the shifting in time, for input-signal causes an unpredictable change in transform coefficients. It has been observed that the standard DWT is seriously disadvantaged by the shift sensitivity that arises from down samplers in the DWT implementation. Shift sensitivity is an undesirable property because it implies that DWT coefficients fail to distinguish between input signal shifts. The shift variant nature of DWT is demonstrated with three shifted step-inputs in Fig. 10. In this figure, input shifted signals are decomposed up to $j = 4$ levels using 'db5'. It shows the unpredictable variations in the reconstructed detail signal at various levels and in final approximation.

2. Poor Directionality

An m - Dimensional transform ($m > 1$) suffers poor directionality when the transform coefficients reveal only a few feature orientations in the spatial domain. The separable 2-D DWT partitions the frequency domain into three directional subbands. 2-D DWT can resolve only three spatial-domain feature orientations: horizontal (HL), vertical (LH) and diagonal (HH). Natural images contain number of smooth regions and edges with random orientations; hence poor directionality affects the optimal representation of natural images with of the separable standard 2-D DWT.

II(b).Dual Tree complex wavelet transform(DTCWT)

As the name reflects, the Dual Tree Complex Wavelet Transform is the one with two trees, each containing a complex valued filter banks. The implementation of such a transform is done using two mother wavelets, one for each tree, one of them being (approximately) the Hilbert transform of the other. On one hand, the dual-tree DWT can be viewed as an overcomplete wavelet transform with a redundancy factor of two. On the other hand, the dual-tree DWT is also a complex DWT, where the first and second DWTs represent the real and imaginary parts of a single complex DWT [6–7]. Fig.6 shows the filter bank representation of DTCWT decomposition. For the filter bank structure, shown in Fig 6, let h_0 and h_1 represent CQF (Conjugate Quadrature Filter) pair [8–10]. That is,

$$h_1(n) = (-1)^n h_0(1 - n)$$

and in Z-transform domain

$$H_0(z)H_0(z^{-1}) + H_1(z)H_1(z^{-1}) = 2$$

$$H_1(z) = z^{-1}H_0(z^{-1})$$

The real tree and imaginary tree scaling and wavelet functions form the Hilbert Transform pairs.

If $\varphi_h(t), \psi_h(t), \varphi_g(t)$ and $\psi_g(t)$ are the scaling and wavelet functions of real and imaginary trees,

the relation between the real and imaginary scaling and wavelet functions is given by

$$\left. \begin{aligned} \varphi_g(t) &= \mathbf{H}\{\varphi_h(t)\} \\ \psi_g(t) &= \mathbf{H}\{\psi_h(t)\} \end{aligned} \right\}$$

DTCWT has approximate shift-invariance, or in other words, improved time-shift sensitivity in comparison with standard DWT. The reconstructed details at various levels and approximation at the last level have almost uniform shifts for the time-shifted unit step functions [10]. The shift sensitive nature of DTCWT is illustrated in the Fig.10. and from these figures, it is obvious that the shift sensitivity of real DWT is poorer than that of DTCWT.

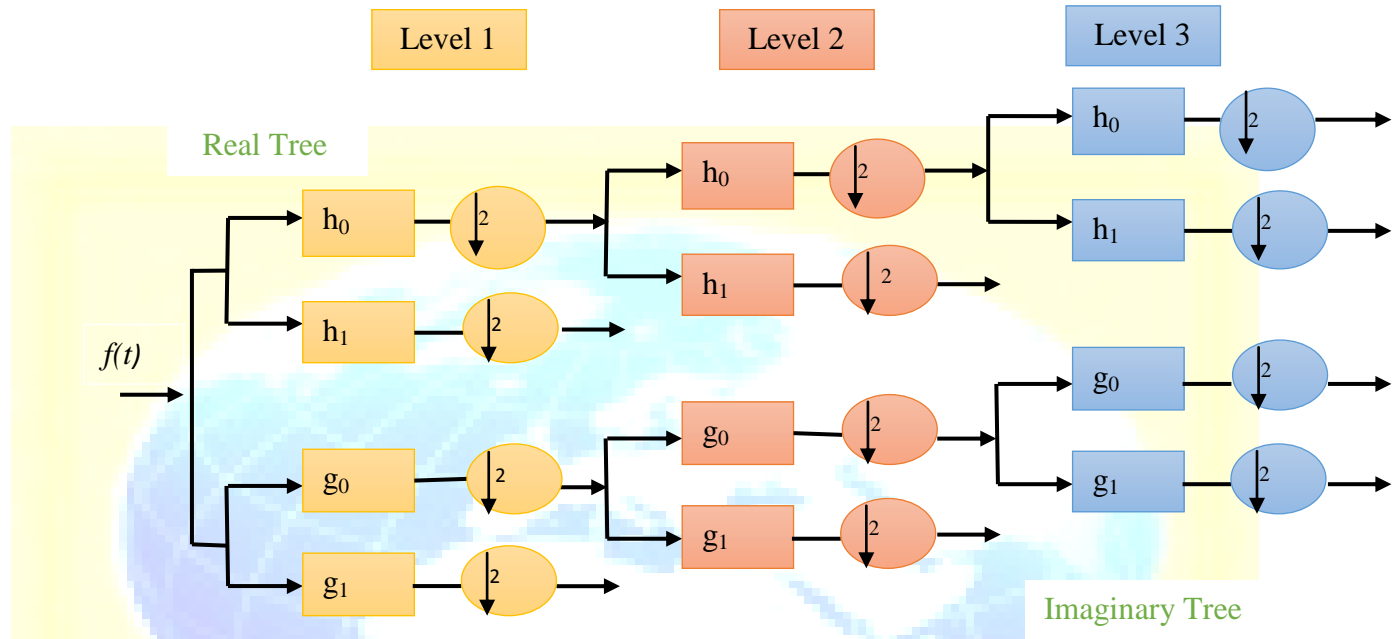


Fig 6. Analysis Filter Bank of DTCWT

11(c).Hyperanalytic Wavelet Transform(HWT)

In Dual Tree Complex Wavelet Transform, one is required to design the low pass, high pass FIR filters for both real tree and imaginary tree, such that the scaling and wavelet functions of real and imaginary trees form a Hilbert Transform pair. It means, that the filters of DTCWT are designed with some more constraints than in the filters of classical wavelet transforms. Instead of designing the complex filters which is not easy task, it is better to process the complex signal or image (Analyticity) corresponding to the given signal or image, using classical wavelets.

Given a real signal $x(t)$ we can construct the complex (analytic) signal as

$$z(t) = x(t) + j H\{x(t)\}$$

The implementation of complex wavelet transform of the signal $x(t)$ is given as

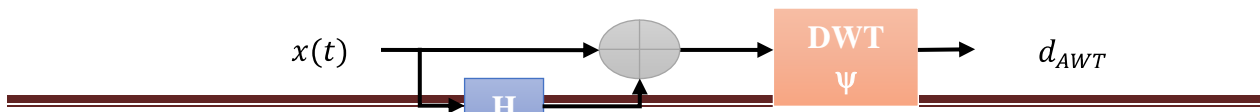


Fig. 7. Implementation of Analytic (Complex) Wavelet Transform (AWT)

From this implementation of AWT [11], the wavelet coefficients of ADWT as follow,

$$d_{AWT} = \langle x_a(t), \psi_n(t) \rangle$$

$$= \langle x(t) + jH\{x(t)\}, \psi_n(t) \rangle.$$

Where $x_a(t)$ is the analytic (complex) signal corresponding $x_a(t)$, $\psi_n(t)$ is the classical wavelet. For one dimensional signal, the analytic signal can be computed with the help of Hilbert Transform along the length of the signal. But, for 2D-signal like image, its analytic signal is computed by finding the Hilbert Transform along the rows, columns and both rows and columns of the image. The two dimensional implementation of Analytic Wavelet Transform is called Hyperanalytic Wavelet Transform (HWT).

The hypercomplex mother wavelet associated to the real mother wavelet, $\psi(x, y)$ is defined as:

$$\psi_a(x, y) = \psi(x, y) + iH_x\{\psi(x, y)\} + jH_y\{\psi(x, y)\} + kH_x\{H_y\{\psi(x, y)\}\}$$

The Hyperanalytic Wavelet Transform (HWT) [11 – 13] of an image $f(x, y)$ is

$$HWT\{f(x, y)\} = \langle f(x, y), \psi(x, y) \rangle + \langle f(x, y), iH_x\{\psi(x, y)\} \rangle + \langle f(x, y), jH_y\{\psi(x, y)\} \rangle$$

$$+ \langle f(x, y), kH_x\{H_y\{\psi(x, y)\}\} \rangle$$

where, $i^2 = j^2 = k^2 = ijk = -1, ij = -ji = k, jk = -kj = i, \text{ and } ki = -ik = j$

$$\Rightarrow \langle f(x, y), \psi(x, y) \rangle + i\langle H_x\{f(x, y)\}, \psi(x, y) \rangle + \langle f(x, y), jH_y\{\psi(x, y)\} \rangle$$

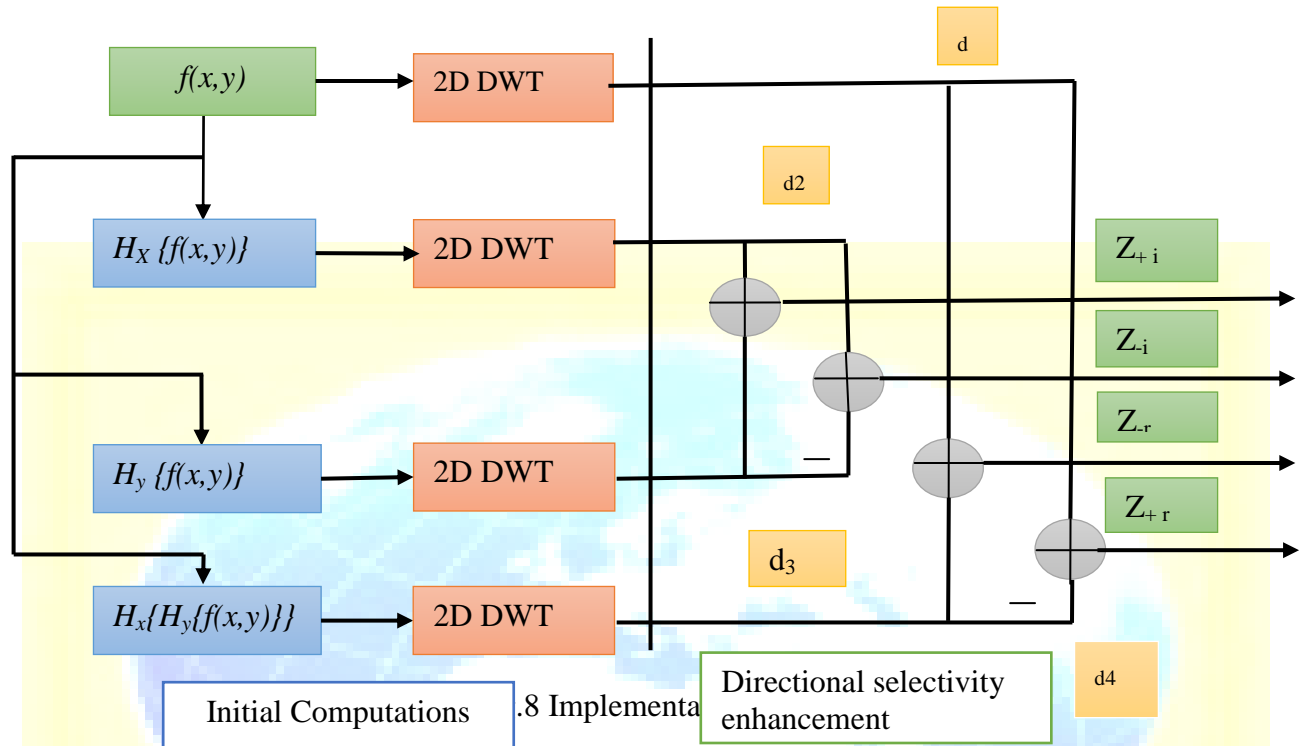
$$+ \langle f(x, y), kH_x\{H_y\{\psi(x, y)\}\} \rangle$$

$$HWT\{f(x, y)\} = DWT\{f(x, y)\} + iDWT\{H_x\{f(x, y)\}\} + jDWT\{H_y\{f(x, y)\}\}$$

$$+ kDWT\{H_x\{H_y\{f(x, y)\}\}\} \Rightarrow \langle f_a(x, y), \psi(x, y) \rangle = DWT\{f_a(x, y)\}$$

The HWT of the image $f(x, y)$ can be computed with the aid of the 2D DWT of its associated hyper complex image. In consequence the HWT implementation uses four trees, each one implementing a 2D DWT, thus having a redundancy of four. The first tree is applied to the input image. The second and the third trees are applied to 1D Hilbert transforms computed across the lines (H_x) or columns (H_y) of the input image. The fourth tree is applied to the result obtained

after the computation of the two 1D Hilbert transforms of the input image. The HWT implementation is presented in Fig.8.



II (d).Hyperanalytic Dual Tree Complex Wavelet Transform (HDTCWT) (proposed method)

Hyperanalytic Dual Tree Complex Wavelet Transform (HDTCWT) is obtained by mixing the key features of the both HWT and DTCWT. The details of HWT provides the information about the pixels oriented in $\pm \tan^{-1}(1/2)$, $\pm \tan^{-1}(2)$ and $\pm \pi/4$. In the case of DTCWT, one can obtain the information about the pixels oriented in the $\pm \pi/12$, $\pm 5\pi/12$ and $\pm \pi/4$. It means that HWT effectively denoise the images with orientations $\pm \tan^{-1}(1/2)$, $\pm \tan^{-1}(2)$ and $\pm \pi/4$ and DTCWT excels in denoising the images with orientations $\pm \pi/12$, $\pm 5\pi/12$ and $\pm \pi/4$. In the case of HDTCWT, one can obtain the both the features simultaneously, and hence, the HDTCWT technique performs better than the HWT and the DTCWT techniques.

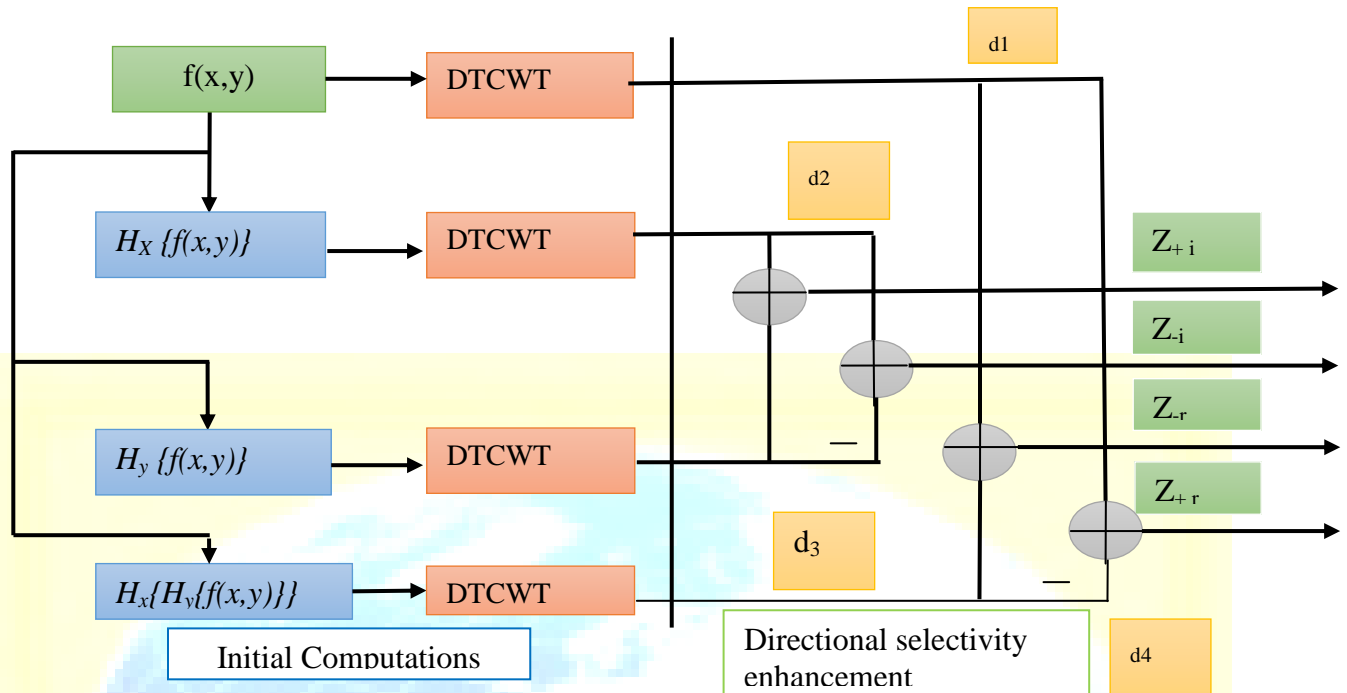


Fig .9. Implementation of HDTTCWT

The implementation of HDTTCWT is shown in the Fig.9. The realization of HDTTCWT is similar to that of HWT but the difference is the using of DTCWT instead of DWT as in HWT. The realization of HDTTCWT is accomplished in the following steps:

1. Constructing the Hyperanalytic image (signal) corresponding to the given image, which consists of the original image $f(x, y)$, image with Hilbert Transform computed along the rows $H_x\{f(x, y)\}$ image with Hilbert Transform with Hilbert Transform performed along the columns $H_y\{f(x, y)\}$ and image with Hilbert Transform computed along both the rows and columns of the image $H_x\{H_y\{f(x, y)\}\}$.
2. Applying the DTCWT over each of the Hyperanalytic image.
3. Obtain the Approximation and Details separately of the four DTCWTs for further processing

Advantages of Complex Wavelet Transforms:

Complex Wavelet Transform provides better shift invariance and good directional enhancement [14, 15] compared to the Discrete Wavelet Transform. These are illustrated clearly in the following sections.

1. Shift Invariance:

The quasi-shift invariance nature of the different wavelet transform techniques are shown in the Fig.10. From this figure, it is obvious that the complex wavelet transforms ADWT (HWT), DTCWT, ADTCWT (HDTTCWT) provides near shift invariance when compared to classical DWT.

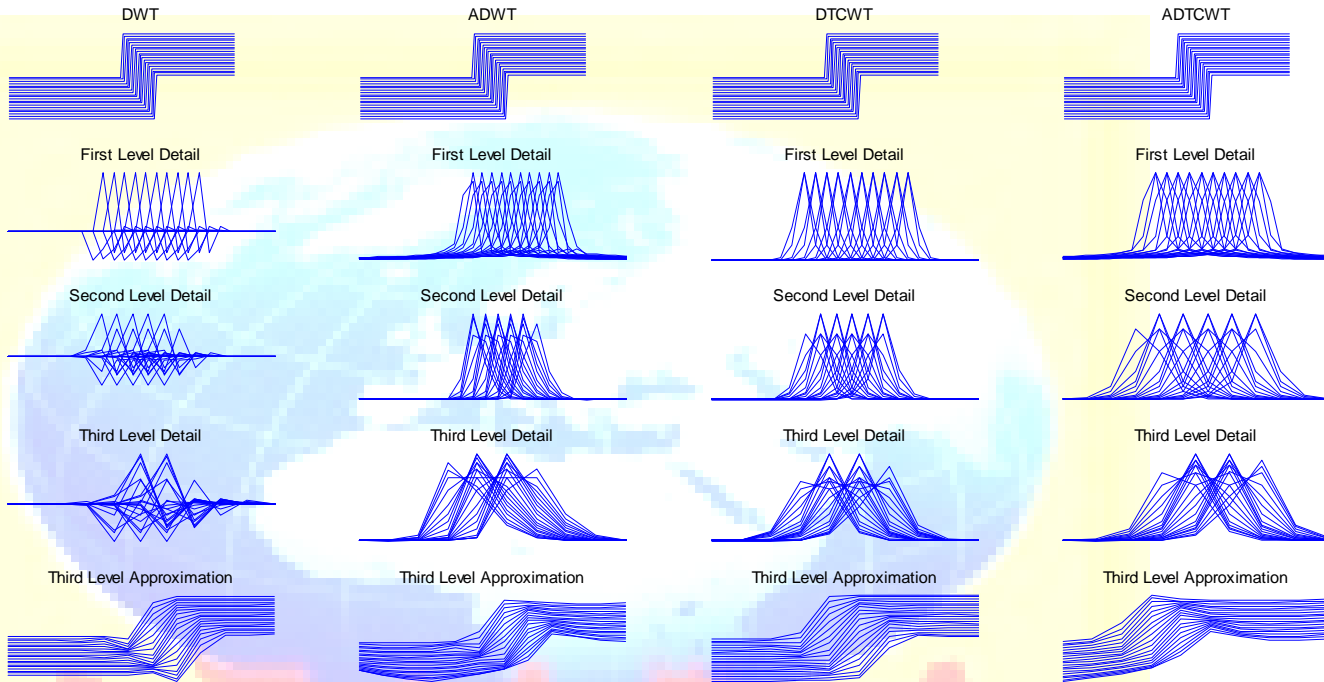


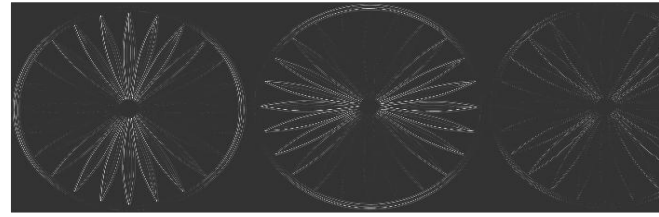
Fig.10. The quasi-shift invariance nature of the different wavelet transform techniques

2 Directional Selectivity:

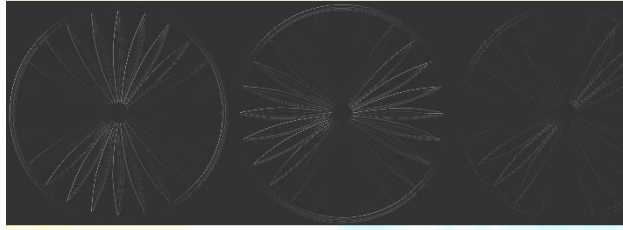
The classical DWT provide information about the 0^0 , 90^0 , $\pm 45^0$ directions only, also, DWT cannot discriminate the $+ 45^0$ and $- 45^0$ orientations in the diagonals. This poor directionality present in DWT is drastically reduced by employing the complex wavelet transform. The following Fig.11& Table.1 shows the directionality features of the different wavelet transforms. From these figures, it is evident that the complex wavelet transforms are capable of discriminating the positive and negative orientations.



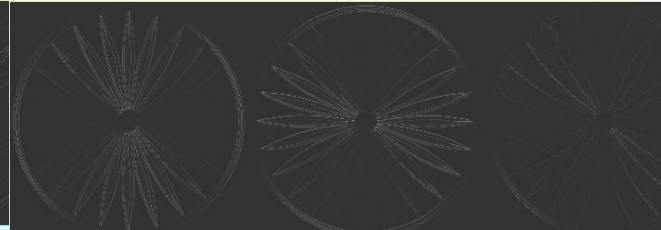
Original Image



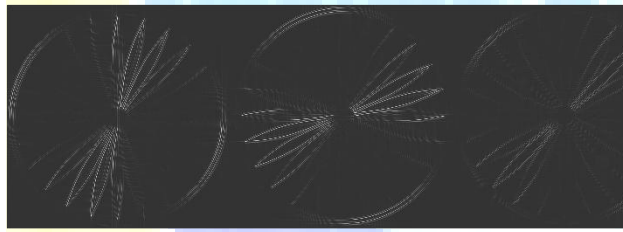
DWT (90° , 0° or 180° and $\pm 45^\circ$)



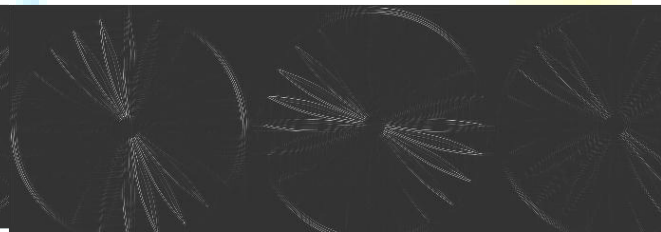
DTCWT (75° , 15° and 45°)



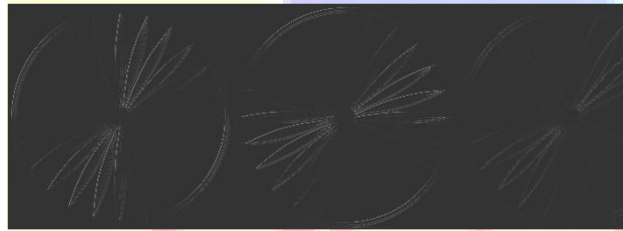
DTCWT (-75° , -15° and -45°)



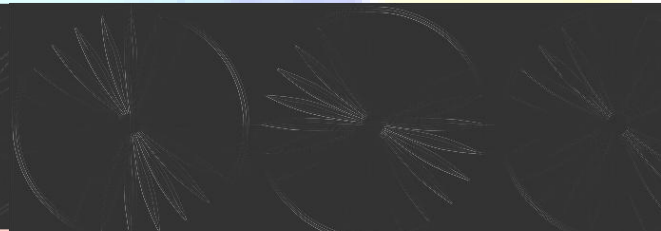
HWT ($\tan^{-1}(2)$, $\tan^{-1}(1/2)$, and 45°)



HWT ($-\tan^{-1}(2)$, $-\tan^{-1}(1/2)$, and -45°)



HDCWT (60° , 30° , 45°)



HDCWT (-60° , -30° , -45°)

Fig.11. shows the directionality features of the different wavelet transforms

Wavelet Transforms	Horizontal	Vertical	Diagonal
DWT	0°	90°	$\pm 45^\circ$
HWT	26.56°	63.44°	45°
	-26.56°	-63.44°	-45°
DTCWT	15°	75°	45°
	-15°	-75°	-45°

HDTCWT	30^0	60^0	45^0
	-30^0	-60^0	-45^0

Table.1 for Directional Selectivity

III. IMAGE DENOISING

Image denoising algorithms are often used to enhance the quality of the images by suppressing the noise level while preserving the significant aspects of interest in the image. Several methods are proposed in literature for image denoising, where Discrete Wavelet Transform-Domain filters are very popular. A wavelet transform is the representation of a function by wavelets. The wavelets are scaled and translated copies (known as daughter wavelets) of a finite length or fast decaying oscillating waveform. A wavelet transform is classified into continuous wavelet transform (CWT) and DWT. The continuous wavelet transform (CWT) has received significant attention for its ability to perform a time-scale analysis of signals. On the other hand, the discrete wavelet transform (DWT) is an implementation of the wavelet transform using a discrete set of wavelet scales and translations obeying some definite rules. In other words, this transform decomposes the signals into mutually orthogonal set of wavelets. In this paper we only discuss methods based on DWT. Recently, a lot of methods have been reported that perform denoising in DWT-domain. The transform coefficients within the sub bands of a DWT can be locally modeled as Independent Identically Distributed (IID) random variables with generalized Gaussian distribution.

Bi-shrink Filter:

In this paper, the denoising technique is implemented using HDTCWT. The wavelet coefficients are filtered using bivariate shrinkage technique [16–18]. With the help of Bayesian estimation theory we are using a simple non-linear shrinkage function for wavelet denoising, which generalizes the Soft Thresholding [19] approach of Donoho and Johnstone. The new shrinkage function, which depends on both the coefficient and its parent, yields improved results for wavelet-based image denoising.

Let w_2 represent the parent of w_1 (w_2 is the wavelet coefficient at the same spatial position as w_1 but at the next coarser scale).

$$\text{Then } y = w + n$$

Where $w = w_1 + w_2$, $y = y_1 + y_2$ and $n = n_1 + n_2$. The noise values n_1, n_2 are zero-mean Gaussian with variance σ^2 . Based on the empirical histograms that we have computed, we propose the following non-Gaussian bivariate [16 – 18] Probability Density Function (pdf)

$$P_w(w) = \frac{3}{2\pi\sigma^2} \exp\left(-\frac{\sqrt{3}}{\sigma} \sqrt{w_1^2 + w_2^2}\right)$$

With this pdf, w_1 and w_2 are uncorrelated, but not independent. The MAP estimator of w_1 yields the following bivariate shrinkage function

$$\hat{W}_1 = \frac{(\sqrt{y_1^2 + y_2^2} - \frac{\sqrt{3}\sigma_n^2}{\sigma})_+}{\sqrt{y_1^2 + y_2^2}} \cdot y_1$$

For this bivariate shrinkage function, the smaller the parent value, the greater the shrinkage.

By adding the features of HWT and DTCWT, the proposed technique HDTCWT performs well in the image denoising compared to the HWT and DTCWT based image denoising techniques

The algorithm of this work is

1. Consider an original Image (noise free)
2. Generate the noisy images (Gaussian) with different values of standard deviation
3. For noisy image, apply DWT, DTCWT, HWT and HDTCWT techniques.
4. Filter the detail coefficients of all DWT, DTCWT, HWT and HDTCWT using bivariate shrinkage technique.
5. Apply the inverse DWT, DTCWT, HWT and HDTCWT for the filtered coefficients to get denoised images.
6. Compute the Mean Square Error (MSE) and Peak Signal to Noise Ratio (PSNR) of the denoised images with respect to the original image
7. Tabulate the MSE and PSNR for different amount of noises, for different wavelet techniques.

The Mean Square Error (MSE) is calculated by using the following equation,

$$MSE = \frac{\sum_{m=1, n=1}^{M, N} |I_o(m, n) - I_i(m, n)|^2}{M \cdot N}$$

where, $I_i(m,n)$ is the input, noise free image, $I_o(m,n)$ is the output image, may be noisy or denoised, and M, N are the number of rows and columns of the image, respectively.

The Peak Signal to Noise Ratio (PSNR) is being computed using the following equation,

$$PSNR = 10 \log_{10} \left(\frac{R^2}{MSE} \right)$$

where, R is the maximum fluctuation in the input image data type. For example, if the input image has a double-precision floating-point data type, then R is 1. If it has an 8-bit unsigned integer data type, R is 255.

IV. Results and Discussion

The performance of the proposed technique is assessed by comparing with DTCWT and HWT based image denoising techniques, for the 'Lena' image of dimensions 512 x 512, for Gaussian noise with standard deviation varying from 10 to 100 in steps of 10. HWT based techniques uses 'sym5' wavelet filters, for wavelet decomposition and reconstruction, because these particular wavelets suits well to this 'Lena' image. The proposed technique HDCWT uses the DTCWT filters for wavelet decomposition and reconstruction

The details coefficients of the each stage are filtered using bivariate shrinkage technique. The denoised images using DWT, DTCWT, HWT and HDCWT are shown in the Fig 12 (a), 12 (b), 12 (c), 12 (d), 12 (e) and Fig.12 (f) respectively. For graphical interpretation, MSE and PSNR values are represented as bar graphs for the different values of σ shown in Fig13 (a) and 13(b). The performance metrics MSE and PSNR are tabulated in the Tables 2 and 3 respectively.

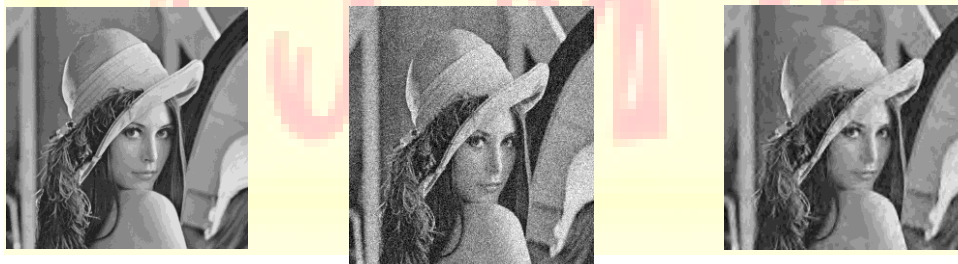


Fig.12(a)Original Image Fig.12(b)Noisy Image ($\sigma = 40$) Fig.12(c)Denoising using DWT (sym5)



Fig.12(d)Denoised using HWT (sym5)



Fig.12(e)Denoised using DTCWT



Fig.12(f) Denoised using HDTCWT

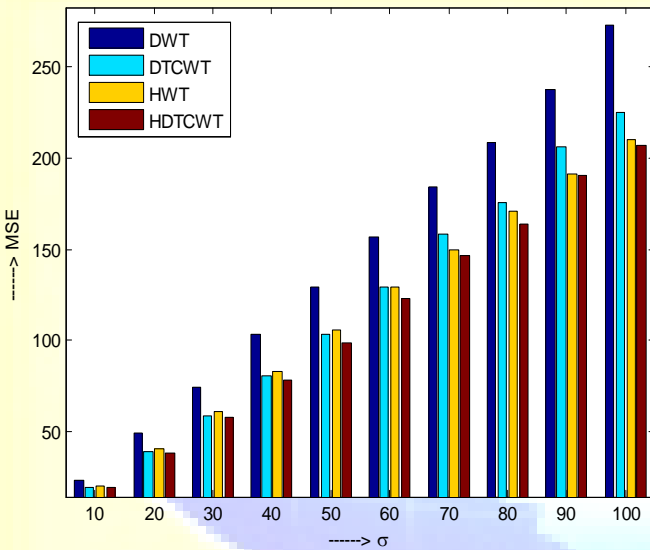


Fig13 (a). Variation of MSE of different techniques for different values of σ

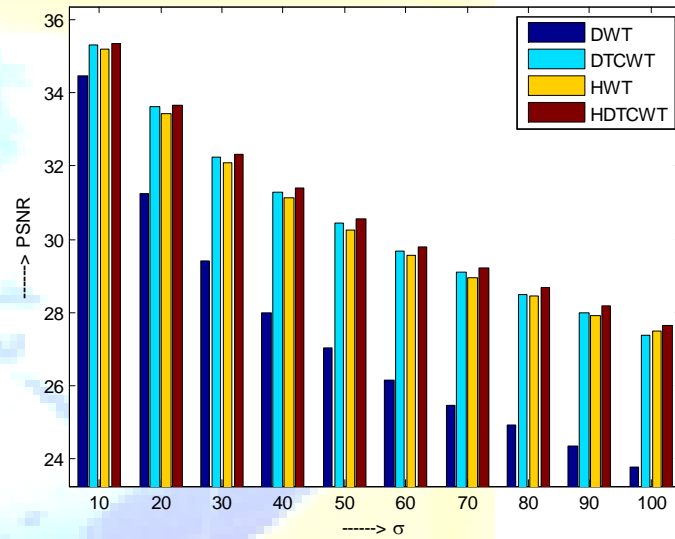


Fig13(b)Variation of PSNR of different techniques for different values of σ

σ	10	20	30	40	50	60	70	80	90	100
Noisy	100	400	900	1600	2500	3600	4900	6400	8100	10000
DWT	23.23	48.87	74.46	102.99	128.85	156.89	183.94	208.99	237.61	272.78
DTCWT	19.15	28.38	38.91	48.54	58.62	70.32	80.18	92.27	103.53	119.15
HWT	19.77	29.52	40.28	50.01	61.11	71.96	82.43	92.91	105.22	115.37
HDTCWT	18.97	27.99	38.11	47.32	57.42	67.93	78.18	87.92	98.87	111.96

Table.2.Comparison of MSE values of the DWT, DTCWT, HWT and HDTCWT techniques for image denoising

σ Type of WT	10	20	30	40	50	60	70	80	90	100
Noisy	28.15	22.11	18.59	16.09	14.14	12.55	11.22	10.07	9.06	8.12
DWT	34.47	31.24	29.41	28.00	27.03	26.17	25.48	24.93	24.37	23.77
DTCWT	35.31	32.23	30.45	29.09	27.98	27.01	26.13	25.69	24.99	24.61
HWT	35.17	32.08	30.27	28.97	27.91	27.03	26.38	25.81	25.31	24.90
HDTCWT	35.35	32.32	30.54	29.20	28.18	27.24	26.48	25.99	25.33	24.97

Table.3.Comparison of PSNR values of the DWT, DTCWT, HWT and HDTCWT Techniques for image denoising

Observations:

1. At very small level of noises ($\sigma \leq 5$), the techniques are not that much sensitive to the noise.
2. HWT outpaces better than DTCWT with increased noise levels.[19]
3. However, HDTCWT techniques performs better than the HWT and DTCWT irrespective of the noise level, as it combines the features of the both HWT and DTCWT.

V. Conclusion

This paper studies and compares the features such as shift sensitivity and directionality of the different complex wavelet transforms like HWT, DTCWT and HDTCWT. The performances of these wavelet techniques in image denoising is evaluated by using bi-shrink filter technique. Irrespective of the noise level, the HDTCWT based image denoising technique outperform well than the other techniques because of its enhanced directional selectivity.

References

- [1] R.Gomathi & S.Selvakumaran, "A Bivariate Shrinkage Function For Complex Dual Tree DWT Based Image Denoising," In Proc. ICWAMS-2006, Bucharest, Romania, October 16-18, 2006.
- [2] L. Sendur and I.W. Selesnick, "Bivariate shrinkage with local variance estimation," IEEE Signal Processing Letters, 9(12), December 2002.
- [3] L. Sendur and I.W. Selesnick, "Bivariate shrinkage functions for wavelet-based denoising exploiting interscale dependency," IEEE Trans. On Signal Processing, 50(11):2744-2756, Nov2002.

- [4] L. Sendur, I.W. Selesnick, "A bivariate shrinkage function for wavelet-based denoising", IEEE International Conference on Acoustics, Speech, and Signal Processing, 2002.
- [5] Felix Fernandes, "Directional, Shift-insensitive, Complex Wavelet Transforms with Controllable Redundancy", PhD Thesis, Rice University, 2002
- [6] N. Kingsbury, Complex Wavelets for Shift Invariant Analysis and Filtering of Signals, Applied and Comp. Harm. Anal.10, 2001, 234-253.
- [7] N G Kingsbury, A Dual-Tree Complex Wavelet Transform with improved orthogonality and symmetry properties, Proc. IEEE Conf. on Image Processing, Vancouver, September 11-13, 2000, paper 1429.
- [8] Ivan W. Selesnick. The Characterization and Design of Hilbert Transform Pairs of Wavelet Bases. In 2001 Conference on Information Science and Systems, The Johns Hopkins University, 2001
- [9] N. Kingsbury, "Image processing with complex wavelets", Philosophical Transactions of the Royal Society London A 357 no.1760:2543-2560, 1999.
- [10] Ivan W. Selesnick, Richard G. Baraniuk and Nick G. Kingsbury. The Dual-Tree Complex Wavelet Transform, IEEE Signal Processing Magazine, 22(6) : pp. 123-151,2005
- [11] C. Naornita, I. Firoiu, J. Boucher, A. Isar "A New Watermarking Method Based on the use of the Hyperanalytic Wavelet Transform"
- [12] I. Firoiu, C. Naornita, "Image Denoising using a New Implementation of Hyperanalytic Wavelet Transform", IEEE Trans. on Instrum. And Meas., Vol. 58, no. 8, pp. 2410-2416, 2009
- [13] I. Adam, C. Naornita, J-M Boucher and A. Isar, "A Bayesian Approach of Hyperanalytic Wavelet Transform Based Denoising".
- [14] I. Adam, C. Naornita, J-M Boucher and A. Isar, "A New Implementation of the Hyperanalytic Wavelet Transform", Proc. of IEEE Sympo. ISSCS 2007, Iasi,Romania, 401– 404.
- [15] I. Firoiu, A. Isar and J. Boucher "An improved version of the Inverse HWT.
- [16] L.Sendur and I.W.Selesnick,"Bivariate shrinkage functions for wavelet-based denoising exploiting

inter scale dependency”, IEEE Trans. Vol. 50 no. 11, pp. 2744-2756, 2002

[17] I. Firoiu, A. Isar, and D. Isar, “A maximum A Posteriori Approach of Hyperanalytic Wavelet Based

Image Denoising in a Multi-Wavelet Content”.

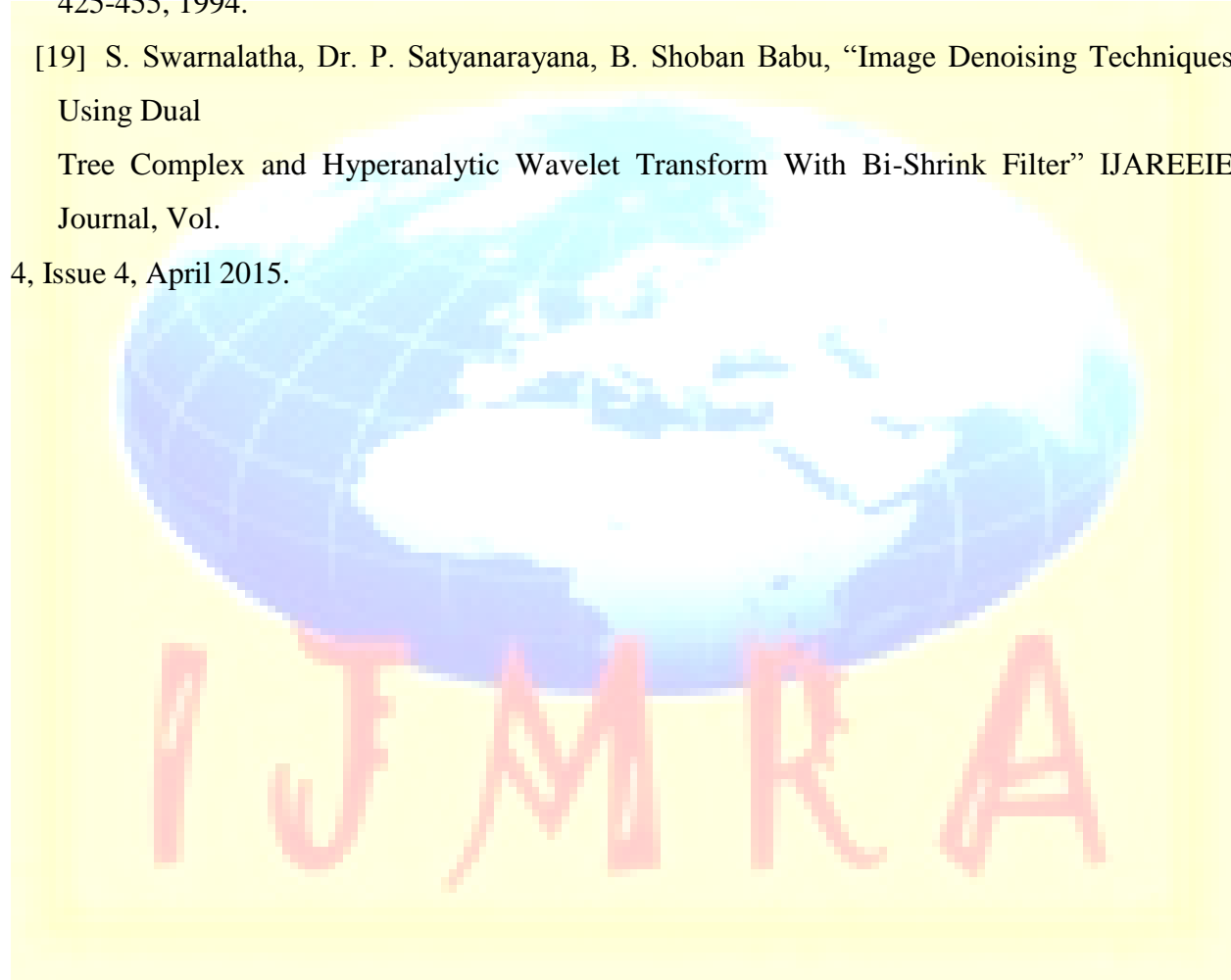
[18] D.L.Donoho, I.M.Johnstone, Ideal spatial adaptation by wavelet shrinkage, Biometrika, 81(3): pp.

425-455, 1994.

[19] S. Swarnalatha, Dr. P. Satyanarayana, B. Shoban Babu, “Image Denoising Techniques Using Dual

Tree Complex and Hyperanalytic Wavelet Transform With Bi-Shrink Filter” IJAREEIE Journal, Vol.

4, Issue 4, April 2015.



Author's profile:-

Mrs S. Swarnalatha received her Bachelor's Degree in Electronics and Communication Engineering from JNTUCEA (JNTU) in 2000, received Master's Degree in Digital Electronics and Communication Systems from JNTUCEA (JNTU) in 2004 and Pursuing Ph.D. from SVUCE (SVU) Tirupati in the Image Processing Domain. Worked as Lecturer at JNTUCEA, Anantapur For 4 Years, as Assistant and Associate Professor in the Department Of ECE, at MITS, Madanapalle, as Associate Professor at CMRIT, Hyderabad and Presently Working as Associate Professor at SVUCE (SVU), Tirupati. Email: swarnasvu09@gmail.com.



Prof. P. Satyanarayana received his Bachelor's Degree in Electronics and Communication Engineering from SVUCE (SVU) in 1976, He received his Master's Degree in Instrumentation and Control System from SVUCE (SVU) in 1978 and he received his Doctorate in Digital Signal Processing 1987 From SVUCE (SVU) in 1987. He is The Post-Doctoral Fellow in Department of Electrical & Computer Engineering at Concordia University, Montreal, Canada During 1988 To 1990. He Worked As Visiting Faculty In The School Of Aerospace Engineering, University Science Malaysia, Pinang, Malaysia From 2004 To 2007. He Visited Number Countries Like USA, Canada, Malaysia, Singapore, And England To Have Academic And Cultural Exchange. He Started His Career As Lecturer From 1976 With The Home University SVUCE (SVU), As Associate Professor During 1991-1999, As Professor During 1999-2013 In Department Of Electronics And Communication Engineering, Tirupati And Presently Working As Professor In ECE at AITS, Tirupati.



Mr B. Shoban Babu received His Graduation Degree in Electronics and Communication Engineering from JNTUCEA (JNTU) in 1998, Master's Degree in Digital Electronics and Communication Systems from MCE (VTU) in the Year 2003, and Pursuing Ph.D. From SVUCE (SVU), Tirupati in the Image Processing Domain. He Worked as Assistant and Associate Professor At MITS, Madanapalle, as Associate Professor at PRIT, Vargal, Hyderabad and Presently Working as Associate Professor at SVCET, Chittoor. Email: bshobanbabu@gmail.com.